Supplemental Material

This supplemental material includes additional information to that already provided in the main letter. A full set of results for the nominal analysis is presented in both graphical and tabular form in Sec. 1. A complete description of the corresponding systematic uncertainties is given in Sec. 2. The correlations between the angular observables are presented for the S_i observables in Sec. 3 and for the $P_i^{(\prime)}$ observables in Sec. 4. The angular and mass distributions of the selected candidates in the different q^2 bins are shown in Sec. 5.

1 Results

The values of S_3, S_4 and S_7–S_9 obtained from the simultaneous fit are shown in Fig. 1. The data are compared to theoretical predictions based on the prescription of Ref. [1]. The predictions combine light-cone sum rule calculations [2] with lattice determinations [3,4] of the $B^0 \to K^{*0}$ form factors. Figure 2 shows the values of the optimised observables, $P_i^{(\prime)}$, obtained from the fit. The data are compared to predictions based on the prescription in Ref. [5]. These predictions use form factors from Ref. [6]. The values of the observables in the standard and optimised basis are given in Tables 1 and 2, respectively. The statistical correlation between the observables in each q^2 bin is provided in Tables 4–13 and Tables 14–23.

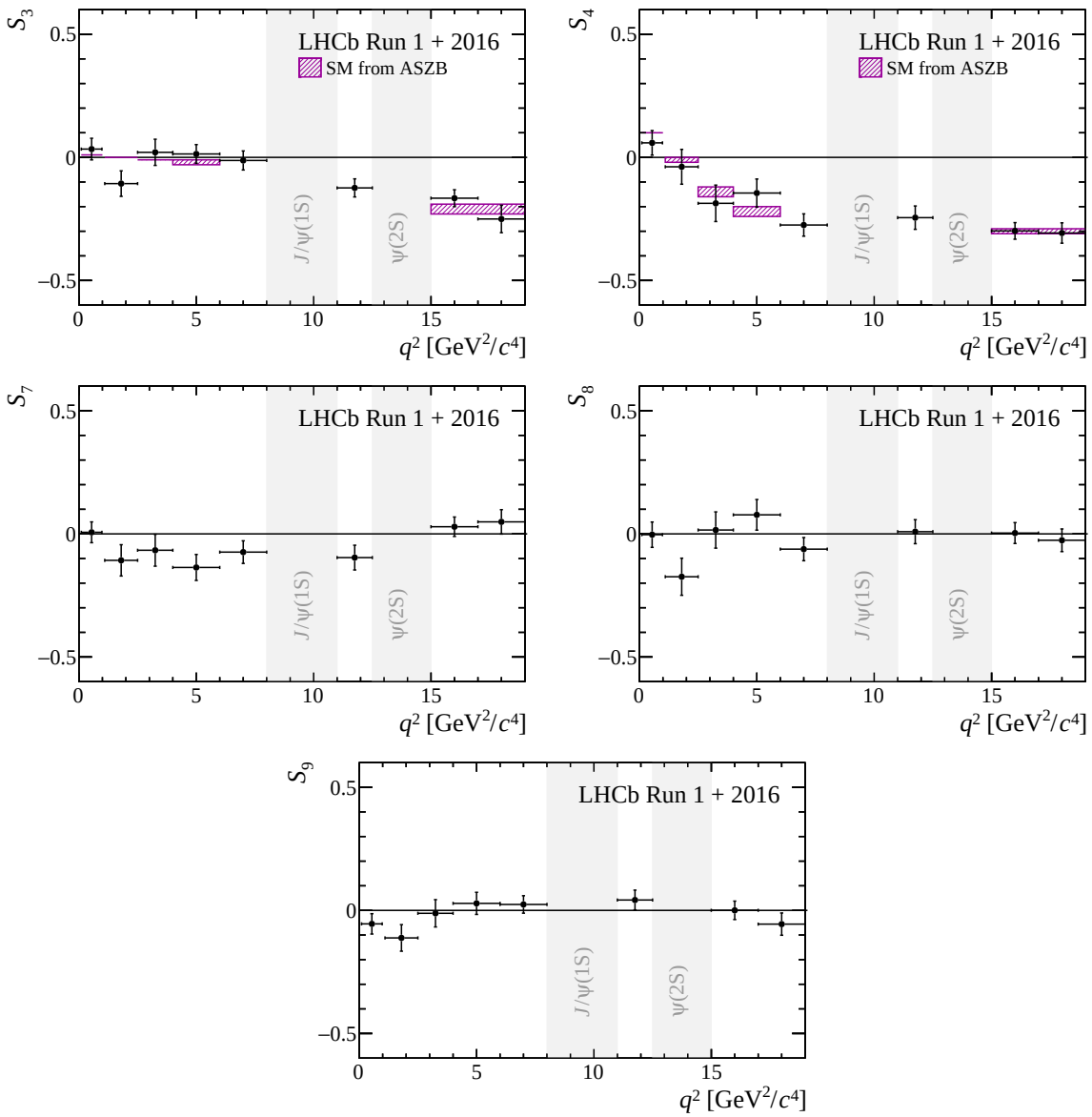

Figure 1: Results for the *CP*-averaged angular observables S_3, S_4 and S_7–S_9 in bins of q^2. The data are compared to SM predictions based on the prescription of Refs. [1, 2].

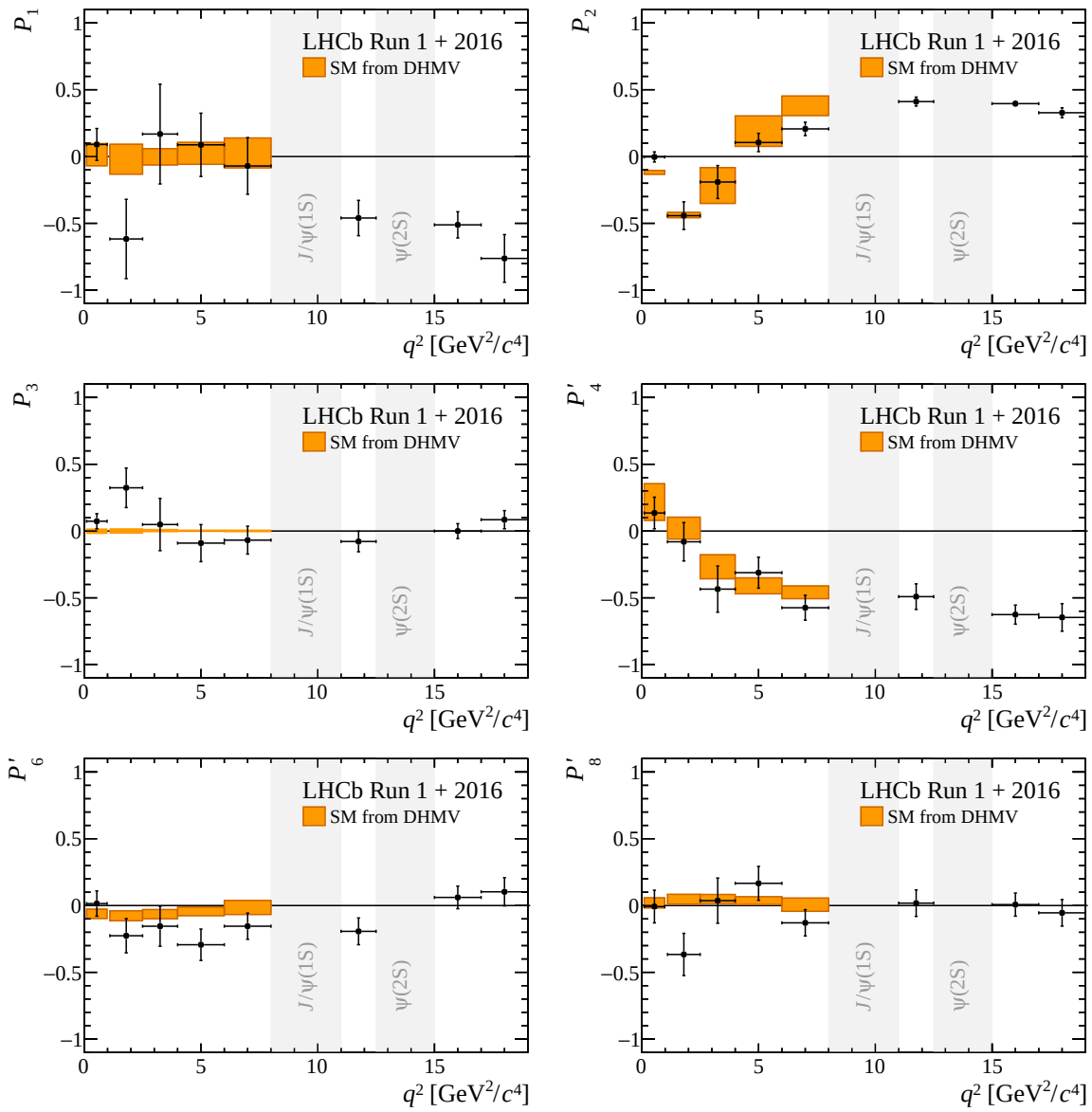

Figure 2: Results for the optimised angular observables P_1–P_3, P'_4, P'_6 and P'_8 in bins of q^2. The data are compared to SM predictions based on Refs. [5, 6].

Table 1: Results for the *CP*-averaged observables $F_{\rm L}$, $A_{\rm FB}$ and S_3–S_9. The first uncertainties are statistical and the second systematic.

$0.10 < q^2 < 0.98\,{\rm GeV}^2/c^4$	
$F_{\rm L}$	$0.255 \pm 0.032 \pm 0.007$
S_3	$0.034 \pm 0.044 \pm 0.003$
S_4	$0.059 \pm 0.050 \pm 0.004$
S_5	$0.227 \pm 0.041 \pm 0.008$
$A_{\rm FB}$	$-0.004 \pm 0.040 \pm 0.004$
S_7	$0.006 \pm 0.042 \pm 0.002$
S_8	$-0.003 \pm 0.051 \pm 0.001$
S_9	$-0.055 \pm 0.041 \pm 0.002$

$1.1 < q^2 < 2.5\,{\rm GeV}^2/c^4$	
$F_{\rm L}$	$0.655 \pm 0.046 \pm 0.017$
S_3	$-0.107 \pm 0.052 \pm 0.003$
S_4	$-0.038 \pm 0.070 \pm 0.011$
S_5	$0.174 \pm 0.060 \pm 0.007$
$A_{\rm FB}$	$-0.229 \pm 0.046 \pm 0.009$
S_7	$-0.107 \pm 0.063 \pm 0.004$
S_8	$-0.174 \pm 0.075 \pm 0.002$
S_9	$-0.112 \pm 0.054 \pm 0.005$

$2.5 < q^2 < 4.0\,{\rm GeV}^2/c^4$	
$F_{\rm L}$	$0.756 \pm 0.047 \pm 0.023$
S_3	$0.020 \pm 0.053 \pm 0.002$
S_4	$-0.187 \pm 0.074 \pm 0.008$
S_5	$-0.064 \pm 0.068 \pm 0.010$
$A_{\rm FB}$	$-0.070 \pm 0.043 \pm 0.006$
S_7	$-0.066 \pm 0.065 \pm 0.004$
S_8	$0.016 \pm 0.074 \pm 0.002$
S_9	$-0.012 \pm 0.055 \pm 0.003$

$4.0 < q^2 < 6.0\,{\rm GeV}^2/c^4$	
$F_{\rm L}$	$0.684 \pm 0.035 \pm 0.015$
S_3	$0.014 \pm 0.038 \pm 0.003$
S_4	$-0.145 \pm 0.057 \pm 0.004$
S_5	$-0.204 \pm 0.051 \pm 0.013$
$A_{\rm FB}$	$0.050 \pm 0.033 \pm 0.002$
S_7	$-0.136 \pm 0.053 \pm 0.002$
S_8	$0.077 \pm 0.062 \pm 0.001$
S_9	$0.029 \pm 0.045 \pm 0.002$

$6.0 < q^2 < 8.0\,{\rm GeV}^2/c^4$	
$F_{\rm L}$	$0.645 \pm 0.030 \pm 0.011$
S_3	$-0.013 \pm 0.038 \pm 0.004$
S_4	$-0.275 \pm 0.045 \pm 0.006$
S_5	$-0.279 \pm 0.043 \pm 0.013$
$A_{\rm FB}$	$0.110 \pm 0.027 \pm 0.005$
S_7	$-0.074 \pm 0.046 \pm 0.003$
S_8	$-0.062 \pm 0.047 \pm 0.001$
S_9	$0.024 \pm 0.035 \pm 0.002$

$11.0 < q^2 < 12.5\,{\rm GeV}^2/c^4$	
$F_{\rm L}$	$0.461 \pm 0.031 \pm 0.010$
S_3	$-0.124 \pm 0.037 \pm 0.003$
S_4	$-0.245 \pm 0.047 \pm 0.007$
S_5	$-0.310 \pm 0.043 \pm 0.011$
$A_{\rm FB}$	$0.333 \pm 0.030 \pm 0.008$
S_7	$-0.096 \pm 0.050 \pm 0.003$
S_8	$0.009 \pm 0.049 \pm 0.001$
S_9	$0.042 \pm 0.040 \pm 0.003$

$15.0 < q^2 < 17.0\,{\rm GeV}^2/c^4$	
$F_{\rm L}$	$0.352 \pm 0.026 \pm 0.009$
S_3	$-0.166 \pm 0.034 \pm 0.007$
S_4	$-0.299 \pm 0.033 \pm 0.008$
S_5	$-0.341 \pm 0.034 \pm 0.009$
$A_{\rm FB}$	$0.385 \pm 0.024 \pm 0.007$
S_7	$0.029 \pm 0.039 \pm 0.001$
S_8	$0.003 \pm 0.042 \pm 0.002$
S_9	$0.000 \pm 0.037 \pm 0.002$

$17.0 < q^2 < 19.0\,{\rm GeV}^2/c^4$	
$F_{\rm L}$	$0.344 \pm 0.032 \pm 0.025$
S_3	$-0.250 \pm 0.050 \pm 0.025$
S_4	$-0.307 \pm 0.041 \pm 0.008$
S_5	$-0.280 \pm 0.040 \pm 0.014$
$A_{\rm FB}$	$0.323 \pm 0.032 \pm 0.019$
S_7	$0.049 \pm 0.049 \pm 0.007$
S_8	$-0.026 \pm 0.046 \pm 0.002$
S_9	$-0.056 \pm 0.045 \pm 0.002$

$1.1 < q^2 < 6.0\,{\rm GeV}^2/c^4$	
$F_{\rm L}$	$0.700 \pm 0.025 \pm 0.013$
S_3	$-0.012 \pm 0.025 \pm 0.003$
S_4	$-0.136 \pm 0.039 \pm 0.003$
S_5	$-0.052 \pm 0.034 \pm 0.007$
$A_{\rm FB}$	$-0.073 \pm 0.021 \pm 0.002$
S_7	$-0.090 \pm 0.034 \pm 0.002$
S_8	$-0.009 \pm 0.037 \pm 0.002$
S_9	$-0.025 \pm 0.026 \pm 0.002$

$15.0 < q^2 < 19.0\,{\rm GeV}^2/c^4$	
$F_{\rm L}$	$0.345 \pm 0.020 \pm 0.007$
S_3	$-0.189 \pm 0.030 \pm 0.009$
S_4	$-0.303 \pm 0.024 \pm 0.008$
S_5	$-0.317 \pm 0.024 \pm 0.011$
$A_{\rm FB}$	$0.353 \pm 0.020 \pm 0.010$
S_7	$0.035 \pm 0.030 \pm 0.003$
S_8	$0.005 \pm 0.031 \pm 0.001$
S_9	$-0.031 \pm 0.029 \pm 0.001$

Table 2: Results for the optimised observables $P_i^{(\prime)}$. The first uncertainties are statistical and the second systematic.

$0.10 < q^2 < 0.98\,\mathrm{GeV}^2/c^4$	
P_1	$0.090 \pm 0.119 \pm 0.009$
P_2	$-0.003 \pm 0.038 \pm 0.003$
P_3	$0.073 \pm 0.057 \pm 0.003$
P_4'	$0.135 \pm 0.118 \pm 0.010$
P_5'	$0.521 \pm 0.095 \pm 0.024$
P_6'	$0.015 \pm 0.094 \pm 0.007$
P_8'	$-0.007 \pm 0.122 \pm 0.002$

$1.1 < q^2 < 2.5\,\mathrm{GeV}^2/c^4$	
P_1	$-0.617 \pm 0.296 \pm 0.023$
P_2	$-0.443 \pm 0.100 \pm 0.027$
P_3	$0.324 \pm 0.147 \pm 0.014$
P_4'	$-0.080 \pm 0.142 \pm 0.019$
P_5'	$0.365 \pm 0.122 \pm 0.013$
P_6'	$-0.226 \pm 0.128 \pm 0.005$
P_8'	$-0.366 \pm 0.158 \pm 0.005$

$2.5 < q^2 < 4.0\,\mathrm{GeV}^2/c^4$	
P_1	$0.168 \pm 0.371 \pm 0.043$
P_2	$-0.191 \pm 0.116 \pm 0.043$
P_3	$0.049 \pm 0.195 \pm 0.014$
P_4'	$-0.435 \pm 0.169 \pm 0.035$
P_5'	$-0.150 \pm 0.144 \pm 0.032$
P_6'	$-0.155 \pm 0.148 \pm 0.024$
P_8'	$0.037 \pm 0.169 \pm 0.007$

$4.0 < q^2 < 6.0\,\mathrm{GeV}^2/c^4$	
P_1	$0.088 \pm 0.235 \pm 0.029$
P_2	$0.105 \pm 0.068 \pm 0.009$
P_3	$-0.090 \pm 0.139 \pm 0.006$
P_4'	$-0.312 \pm 0.115 \pm 0.013$
P_5'	$-0.439 \pm 0.111 \pm 0.036$
P_6'	$-0.293 \pm 0.117 \pm 0.004$
P_8'	$0.166 \pm 0.127 \pm 0.004$

$6.0 < q^2 < 8.0\,\mathrm{GeV}^2/c^4$	
P_1	$-0.071 \pm 0.211 \pm 0.020$
P_2	$0.207 \pm 0.048 \pm 0.013$
P_3	$-0.068 \pm 0.104 \pm 0.007$
P_4'	$-0.574 \pm 0.091 \pm 0.018$
P_5'	$-0.583 \pm 0.090 \pm 0.030$
P_6'	$-0.155 \pm 0.098 \pm 0.009$
P_8'	$-0.129 \pm 0.098 \pm 0.005$

$11.0 < q^2 < 12.5\,\mathrm{GeV}^2/c^4$	
P_1	$-0.460 \pm 0.132 \pm 0.015$
P_2	$0.411 \pm 0.033 \pm 0.008$
P_3	$-0.078 \pm 0.077 \pm 0.007$
P_4'	$-0.491 \pm 0.095 \pm 0.013$
P_5'	$-0.622 \pm 0.088 \pm 0.017$
P_6'	$-0.193 \pm 0.100 \pm 0.003$
P_8'	$0.018 \pm 0.099 \pm 0.009$

$15.0 < q^2 < 17.0\,\mathrm{GeV}^2/c^4$	
P_1	$-0.511 \pm 0.096 \pm 0.020$
P_2	$0.396 \pm 0.022 \pm 0.004$
P_3	$-0.000 \pm 0.056 \pm 0.003$
P_4'	$-0.626 \pm 0.069 \pm 0.018$
P_5'	$-0.714 \pm 0.074 \pm 0.021$
P_6'	$0.061 \pm 0.085 \pm 0.003$
P_8'	$0.007 \pm 0.086 \pm 0.002$

$17.0 < q^2 < 19.0\,\mathrm{GeV}^2/c^4$	
P_1	$-0.763 \pm 0.152 \pm 0.094$
P_2	$0.328 \pm 0.032 \pm 0.017$
P_3	$0.085 \pm 0.068 \pm 0.004$
P_4'	$-0.647 \pm 0.086 \pm 0.057$
P_5'	$-0.590 \pm 0.084 \pm 0.059$
P_6'	$0.103 \pm 0.105 \pm 0.016$
P_8'	$-0.055 \pm 0.099 \pm 0.006$

$1.1 < q^2 < 6.0\,\mathrm{GeV}^2/c^4$	
P_1	$-0.079 \pm 0.159 \pm 0.021$
P_2	$-0.162 \pm 0.050 \pm 0.012$
P_3	$0.085 \pm 0.090 \pm 0.005$
P_4'	$-0.298 \pm 0.087 \pm 0.016$
P_5'	$-0.114 \pm 0.068 \pm 0.026$
P_6'	$-0.197 \pm 0.075 \pm 0.009$
P_8'	$-0.020 \pm 0.089 \pm 0.009$

$15.0 < q^2 < 19.0\,\mathrm{GeV}^2/c^4$	
P_1	$-0.577 \pm 0.090 \pm 0.031$
P_2	$0.359 \pm 0.018 \pm 0.009$
P_3	$0.048 \pm 0.045 \pm 0.002$
P_4'	$-0.638 \pm 0.055 \pm 0.020$
P_5'	$-0.667 \pm 0.053 \pm 0.029$
P_6'	$0.073 \pm 0.067 \pm 0.006$
P_8'	$0.011 \pm 0.069 \pm 0.003$

2 Systematic uncertainties

A summary of the sources of systematic uncertainty on the angular observables is shown in Table 3. Details of how the systematic uncertainties are estimated are given in the letter. The dominant systematic uncertainties arise from the peaking backgrounds that are neglected in the analysis (*peaking backgrounds* in Table 3) and, for the narrow q^2 bins, from the uncertainty associated with evaluating the acceptance at a fixed point in q^2 (*acceptance variation with* q^2 in Table 3). The *bias correction* in Table 3 refers to the biases observed when generating pseudoexperiments using the result of the best fit to data, as discussed in the letter. The systematic uncertainty associated with the *background model* is calculated by increasing the polynomial order to four.

Table 3: Summary of the different sources of systematic uncertainty on the angular observables.

Source	$F_{\rm L}$	$A_{\rm FB}$, S_3–S_9	P_1–P_8'
Acceptance stat. uncertainty	< 0.01	< 0.01	< 0.01
Acceptance polynomial order	< 0.01	< 0.01	< 0.02
Data-simulation differences	< 0.01	< 0.01	< 0.01
Acceptance variation with q^2	< 0.03	< 0.03	< 0.09
$m(K^+\pi^-)$ model	< 0.01	< 0.01	< 0.02
Background model	< 0.01	< 0.01	< 0.03
Peaking backgrounds	< 0.02	< 0.02	< 0.03
$m(K^+\pi^-\mu^+\mu^-)$ model	< 0.01	< 0.01	< 0.02
$K^+\mu^+\mu^-$ veto	< 0.01	< 0.01	< 0.01
Trigger	< 0.01	< 0.01	< 0.01
Bias correction	< 0.02	< 0.02	< 0.04

3 Correlation matrices for the *CP*-averaged observables

Correlation matrices between the *CP*-averaged observables in the different q^2 bins are provided in Tables 4–13. The different q^2 bins are statistically independent.

Table 4: Correlation matrix for the *CP*-averaged observables from the maximum-likelihood fit in the bin $0.10 < q^2 < 0.98\,\mathrm{GeV}^2/c^4$.

	F_L	S_3	S_4	S_5	A_FB	S_7	S_8	S_9
F_L	1.00	−0.00	−0.03	0.09	0.03	−0.01	0.06	0.03
S_3		1.00	0.02	0.14	0.02	−0.06	0.01	−0.01
S_4			1.00	0.06	0.15	−0.03	0.06	0.00
S_5				1.00	0.04	−0.03	−0.01	0.00
A_FB					1.00	−0.02	−0.01	−0.02
S_7						1.00	−0.04	0.10
S_8							1.00	0.02
S_9								1.00

Table 5: Correlation matrix for the *CP*-averaged observables from the maximum-likelihood fit in the bin $1.1 < q^2 < 2.5\,\mathrm{GeV}^2/c^4$.

	F_L	S_3	S_4	S_5	A_FB	S_7	S_8	S_9
F_L	1.00	0.05	0.04	0.16	0.11	−0.08	−0.06	0.05
S_3		1.00	0.00	0.04	0.05	0.08	0.08	0.18
S_4			1.00	−0.20	−0.01	0.02	−0.09	−0.07
S_5				1.00	−0.09	−0.11	−0.02	−0.12
A_FB					1.00	−0.03	0.08	−0.04
S_7						1.00	−0.16	0.14
S_8							1.00	−0.04
S_9								1.00

Table 6: Correlation matrix for the *CP*-averaged observables from the maximum-likelihood fit in the bin $2.5 < q^2 < 4.0\,\mathrm{GeV}^2/c^4$.

	F_L	S_3	S_4	S_5	A_FB	S_7	S_8	S_9
F_L	1.00	−0.02	−0.03	−0.02	−0.03	−0.01	−0.08	0.06
S_3		1.00	−0.05	−0.03	0.05	0.02	−0.07	0.02
S_4			1.00	−0.13	−0.10	0.01	0.03	−0.03
S_5				1.00	−0.08	0.01	0.02	0.03
A_FB					1.00	0.06	−0.05	−0.08
S_7						1.00	0.01	0.03
S_8							1.00	−0.08
S_9								1.00

Table 7: Correlation matrix for the *CP*-averaged observables from the maximum-likelihood fit in the bin $4.0 < q^2 < 6.0\,\mathrm{GeV}^2/c^4$.

	F_L	S_3	S_4	S_5	A_FB	S_7	S_8	S_9
F_L	1.00	−0.01	0.05	−0.02	−0.14	−0.10	0.09	0.04
S_3		1.00	−0.06	−0.10	0.06	−0.02	0.02	−0.08
S_4			1.00	0.01	−0.14	0.03	0.02	0.01
S_5				1.00	−0.08	0.07	0.02	−0.05
A_FB					1.00	−0.01	−0.03	0.01
S_7						1.00	0.03	−0.18
S_8							1.00	−0.00
S_9								1.00

Table 8: Correlation matrix for the *CP*-averaged observables from the maximum-likelihood fit in the bin $6.0 < q^2 < 8.0\,\mathrm{GeV}^2/c^4$.

	F_L	S_3	S_4	S_5	A_FB	S_7	S_8	S_9
F_L	1.00	0.00	−0.01	−0.06	−0.20	−0.05	0.00	−0.06
S_3		1.00	−0.12	−0.24	0.01	0.05	0.04	−0.10
S_4			1.00	0.13	−0.10	0.02	−0.04	−0.04
S_5				1.00	−0.16	−0.01	0.02	−0.06
A_FB					1.00	−0.03	0.02	0.02
S_7						1.00	0.08	−0.09
S_8							1.00	−0.08
S_9								1.00

Table 9: Correlation matrix for the *CP*-averaged observables from the maximum-likelihood fit in the bin $11.0 < q^2 < 12.5\,\mathrm{GeV}^2/c^4$.

	F_L	S_3	S_4	S_5	A_FB	S_7	S_8	S_9
F_L	1.00	0.14	0.02	−0.09	−0.56	0.02	0.01	0.01
S_3		1.00	0.08	−0.08	−0.15	0.02	0.06	−0.10
S_4			1.00	0.08	−0.12	0.03	−0.02	−0.02
S_5				1.00	−0.13	0.03	−0.00	−0.17
A_FB					1.00	−0.05	−0.10	0.12
S_7						1.00	0.27	−0.10
S_8							1.00	−0.01
S_9								1.00

Table 10: Correlation matrix for the *CP*-averaged observables from the maximum-likelihood fit in the bin $15.0 < q^2 < 17.0\,\mathrm{GeV}^2/c^4$.

	F_L	S_3	S_4	S_5	A_FB	S_7	S_8	S_9
F_L	1.00	0.27	0.02	0.07	−0.53	0.00	−0.04	0.06
S_3		1.00	−0.05	0.01	−0.12	−0.02	−0.04	0.10
S_4			1.00	0.29	−0.15	0.02	0.06	0.03
S_5				1.00	−0.28	0.06	0.03	0.04
A_FB					1.00	0.01	−0.00	0.01
S_7						1.00	0.31	−0.23
S_8							1.00	−0.13
S_9								1.00

Table 11: Correlation matrix for the *CP*-averaged observables from the maximum-likelihood fit in the bin $17.0 < q^2 < 19.0\,\mathrm{GeV}^2/c^4$.

	F_L	S_3	S_4	S_5	A_FB	S_7	S_8	S_9
F_L	1.00	0.14	0.06	0.00	−0.35	0.02	−0.02	0.08
S_3		1.00	−0.04	−0.15	−0.12	−0.04	0.03	−0.04
S_4			1.00	0.25	−0.14	−0.10	0.08	0.02
S_5				1.00	−0.25	−0.07	−0.08	0.05
A_FB					1.00	−0.00	−0.03	−0.09
S_7						1.00	0.33	−0.09
S_8							1.00	−0.13
S_9								1.00

Table 12: Correlation matrix for the *CP*-averaged observables from the maximum-likelihood fit in the bin $1.1 < q^2 < 6.0\,\mathrm{GeV}^2/c^4$.

	F_L	S_3	S_4	S_5	A_FB	S_7	S_8	S_9
F_L	1.00	−0.01	−0.02	0.00	0.01	−0.08	0.02	0.03
S_3		1.00	−0.04	−0.01	0.04	0.03	0.00	−0.02
S_4			1.00	−0.07	−0.09	0.01	0.01	−0.03
S_5				1.00	−0.07	0.00	0.01	−0.04
A_FB					1.00	−0.01	−0.03	−0.03
S_7						1.00	−0.02	−0.04
S_8							1.00	−0.08
S_9								1.00

Table 13: Correlation matrix for the *CP*-averaged observables from the maximum-likelihood fit in the bin $15.0 < q^2 < 19.0\,\mathrm{GeV}^2/c^4$.

	F_L	S_3	S_4	S_5	A_FB	S_7	S_8	S_9
F_L	1.00	0.18	−0.06	−0.07	−0.37	0.00	−0.03	0.07
S_3		1.00	−0.04	−0.03	−0.07	−0.00	−0.04	0.02
S_4			1.00	0.21	−0.13	−0.03	0.04	0.06
S_5				1.00	−0.23	0.02	−0.01	0.04
A_FB					1.00	0.03	−0.01	0.00
S_7						1.00	0.28	−0.18
S_8							1.00	−0.14
S_9								1.00

4 Correlation matrices for the optimised angular observables

Correlation matrices between the optimised $P_i^{(\prime)}$ basis of observables in the different q^2 bins are provided in Tables 14–23.

Table 14: Correlation matrix for the optimised angular observables from the maximum-likelihood fit in the bin $0.10 < q^2 < 0.98\,\mathrm{GeV}^2/c^4$.

	F_L	P_1	P_2	P_3	P_4'	P_5'	P_6'	P_8'
F_L	1.00	0.03	0.02	0.03	−0.08	−0.13	−0.02	0.06
P_1		1.00	0.02	0.01	0.02	0.14	−0.06	0.01
P_2			1.00	0.02	0.14	0.03	−0.02	−0.01
P_3				1.00	−0.01	−0.00	−0.10	−0.02
P_4'					1.00	0.07	−0.03	0.06
P_5'						1.00	−0.03	−0.02
P_6'							1.00	−0.04
P_8'								1.00

Table 15: Correlation matrix for the optimised angular observables from the maximum-likelihood fit in the bin $1.1 < q^2 < 2.5\,\mathrm{GeV}^2/c^4$.

	F_L	P_1	P_2	P_3	P_4'	P_5'	P_6'	P_8'
F_L	1.00	−0.23	−0.51	0.26	0.03	0.24	−0.13	−0.13
P_1		1.00	0.15	−0.23	−0.00	−0.02	0.11	0.11
P_2			1.00	−0.09	−0.03	−0.22	0.05	0.14
P_3				1.00	0.07	0.19	−0.17	−0.00
P_4'					1.00	−0.20	0.02	−0.09
P_5'						1.00	−0.12	−0.04
P_6'							1.00	−0.14
P_8'								1.00

Table 16: Correlation matrix for the optimised angular observables from the maximum-likelihood fit in the bin $2.5 < q^2 < 4.0\,\mathrm{GeV}^2/c^4$.

	F_L	P_1	P_2	P_3	P_4'	P_5'	P_6'	P_8'
F_L	1.00	0.08	−0.34	0.01	−0.21	−0.09	−0.08	−0.06
P_1		1.00	0.02	−0.02	−0.07	−0.03	0.00	−0.08
P_2			1.00	0.07	−0.02	−0.05	0.08	−0.03
P_3				1.00	0.02	−0.04	−0.04	0.07
P_4'					1.00	−0.10	0.02	0.04
P_5'						1.00	0.01	0.02
P_6'							1.00	0.01
P_8'								1.00

Table 17: Correlation matrix for the optimised angular observables from the maximum-likelihood fit in the bin $4.0 < q^2 < 6.0\,\mathrm{GeV}^2/c^4$.

	F_L	P_1	P_2	P_3	P_4'	P_5'	P_6'	P_8'
F_L	1.00	0.04	0.05	−0.10	−0.04	−0.14	−0.17	0.14
P_1		1.00	0.06	0.07	−0.06	−0.10	−0.03	0.02
P_2			1.00	−0.02	−0.14	−0.09	−0.03	−0.01
P_3				1.00	−0.01	0.07	0.19	−0.01
P_4'					1.00	0.02	0.04	0.01
P_5'						1.00	0.09	0.00
P_6'							1.00	0.02
P_8'								1.00

Table 18: Correlation matrix for the optimised angular observables from the maximum-likelihood fit in the bin $6.0 < q^2 < 8.0\,\mathrm{GeV}^2/c^4$.

	F_L	P_1	P_2	P_3	P_4'	P_5'	P_6'	P_8'
F_L	1.00	−0.02	0.17	0.01	−0.14	−0.18	−0.08	−0.02
P_1		1.00	0.01	0.10	−0.12	−0.23	0.04	0.04
P_2			1.00	−0.00	−0.13	−0.21	−0.06	0.02
P_3				1.00	0.03	0.06	0.09	0.08
P_4'					1.00	0.15	0.03	−0.03
P_5'						1.00	0.00	0.02
P_6'							1.00	0.08
P_8'								1.00

Table 19: Correlation matrix for the optimised angular observables from the maximum-likelihood fit in the bin $11.0 < q^2 < 12.5\,\mathrm{GeV}^2/c^4$.

	F_L	P_1	P_2	P_3	P_4'	P_5'	P_6'	P_8'
F_L	1.00	−0.07	0.13	−0.07	0.04	−0.07	0.03	0.00
P_1		1.00	−0.09	0.10	0.07	−0.06	0.01	0.05
P_2			1.00	−0.16	−0.12	−0.23	−0.05	−0.11
P_3				1.00	0.01	0.18	0.10	0.00
P_4'					1.00	0.08	0.03	−0.02
P_5'						1.00	0.03	0.00
P_6'							1.00	0.27
P_8'								1.00

Table 20: Correlation matrix for the optimised angular observables from the maximum-likelihood fit in the bin $15.0 < q^2 < 17.0\,\mathrm{GeV}^2/c^4$.

	F_L	P_1	P_2	P_3	P_4'	P_5'	P_6'	P_8'
F_L	1.00	0.06	0.14	−0.06	0.18	0.23	−0.01	−0.04
P_1		1.00	0.03	−0.09	-0.04	0.00	−0.03	−0.04
P_2			1.00	−0.06	−0.13	−0.25	0.01	−0.03
P_3				1.00	−0.04	−0.05	0.23	0.13
P_4'					1.00	0.32	0.02	0.06
P_5'						1.00	0.06	0.03
P_6'							1.00	0.31
P_8'								1.00

Table 21: Correlation matrix for the optimised angular observables from the maximum-likelihood fit in the bin $17.0 < q^2 < 19.0\,\mathrm{GeV}^2/c^4$.

	F_L	P_1	P_2	P_3	P_4'	P_5'	P_6'	P_8'
F_L	1.00	−0.10	0.16	−0.01	0.22	0.14	−0.01	−0.01
P_1		1.00	−0.10	0.05	−0.07	−0.16	−0.05	0.03
P_2			1.00	0.06	−0.09	−0.23	0.00	−0.05
P_3				1.00	−0.01	−0.06	0.09	0.14
P_4'					1.00	0.27	−0.09	0.08
P_5'						1.00	−0.07	−0.09
P_6'							1.00	0.34
P_8'								1.00

Table 22: Correlation matrix for the optimised angular observables from the maximum-likelihood fit in the bin $1.1 < q^2 < 6.0\,\mathrm{GeV}^2/c^4$.

	F_L	P_1	P_2	P_3	P_4'	P_5'	P_6'	P_8'
F_L	1.00	−0.05	−0.33	0.09	−0.11	−0.03	−0.14	0.02
P_1		1.00	0.05	0.02	−0.04	−0.00	0.03	0.01
P_2			1.00	−0.00	−0.04	−0.06	0.03	−0.04
P_3				1.00	0.02	0.03	0.03	0.08
P_4'					1.00	−0.06	0.03	0.01
P_5'						1.00	0.01	0.00
P_6'							1.00	−0.02
P_8'								1.00

Table 23: Correlation matrix for the optimised angular observables from the maximum-likelihood fit in the bin $15.0 < q^2 < 19.0\,\mathrm{GeV}^2/c^4$.

	F_L	P_1	P_2	P_3	P_4'	P_5'	P_6'	P_8'
F_L	1.00	−0.08	0.19	−0.02	0.11	0.09	−0.01	−0.04
P_1		1.00	−0.01	−0.00	−0.04	−0.02	0.00	−0.04
P_2			1.00	−0.04	−0.14	−0.25	0.03	−0.03
P_3				1.00	−0.06	−0.04	0.18	0.14
P_4'					1.00	0.21	−0.03	0.04
P_5'						1.00	0.02	−0.01
P_6'							1.00	0.28
P_8'								1.00

5 Fit projections of the signal channel

The angular and mass distributions of the candidates in bins of q^2 for the Run 1 and the 2016 data, along with the projections of the simultaneous fit, are shown in Figs. 3–12.

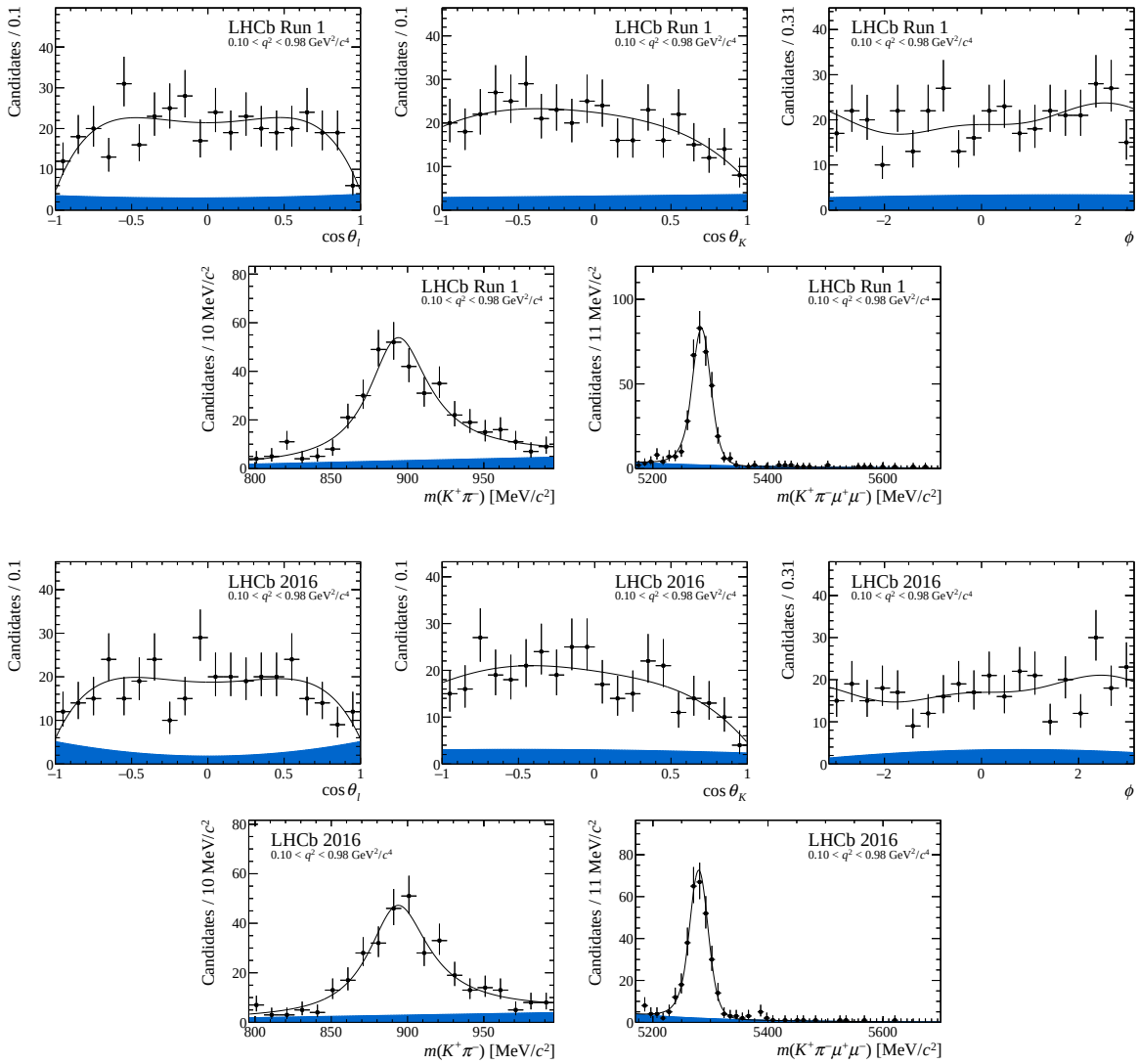

Figure 3: Projections of the fitted probability density function on the decay angles, $m(K^+\pi^-)$ and $m(K^+\pi^-\mu^+\mu^-)$ for the bin $0.10 < q^2 < 0.98\,\mathrm{GeV}^2/c^4$. The blue shaded region indicates background.

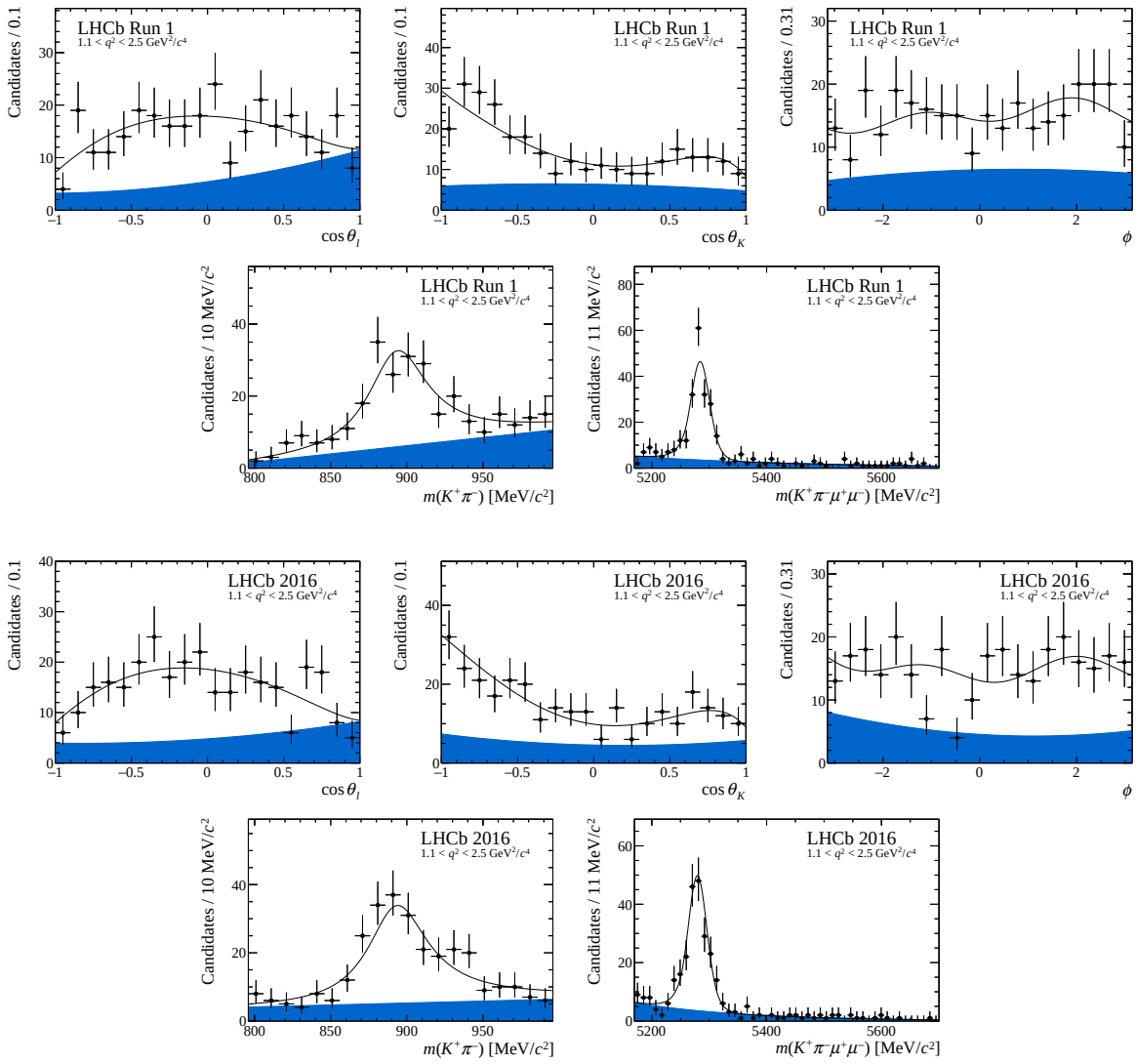

Figure 4: Projections of the fitted probability density function on the decay angles, $m(K^+\pi^-)$ and $m(K^+\pi^-\mu^+\mu^-)$ for the bin $1.1 < q^2 < 2.5\,\mathrm{GeV}^2/c^4$. The blue shaded region indicates background.

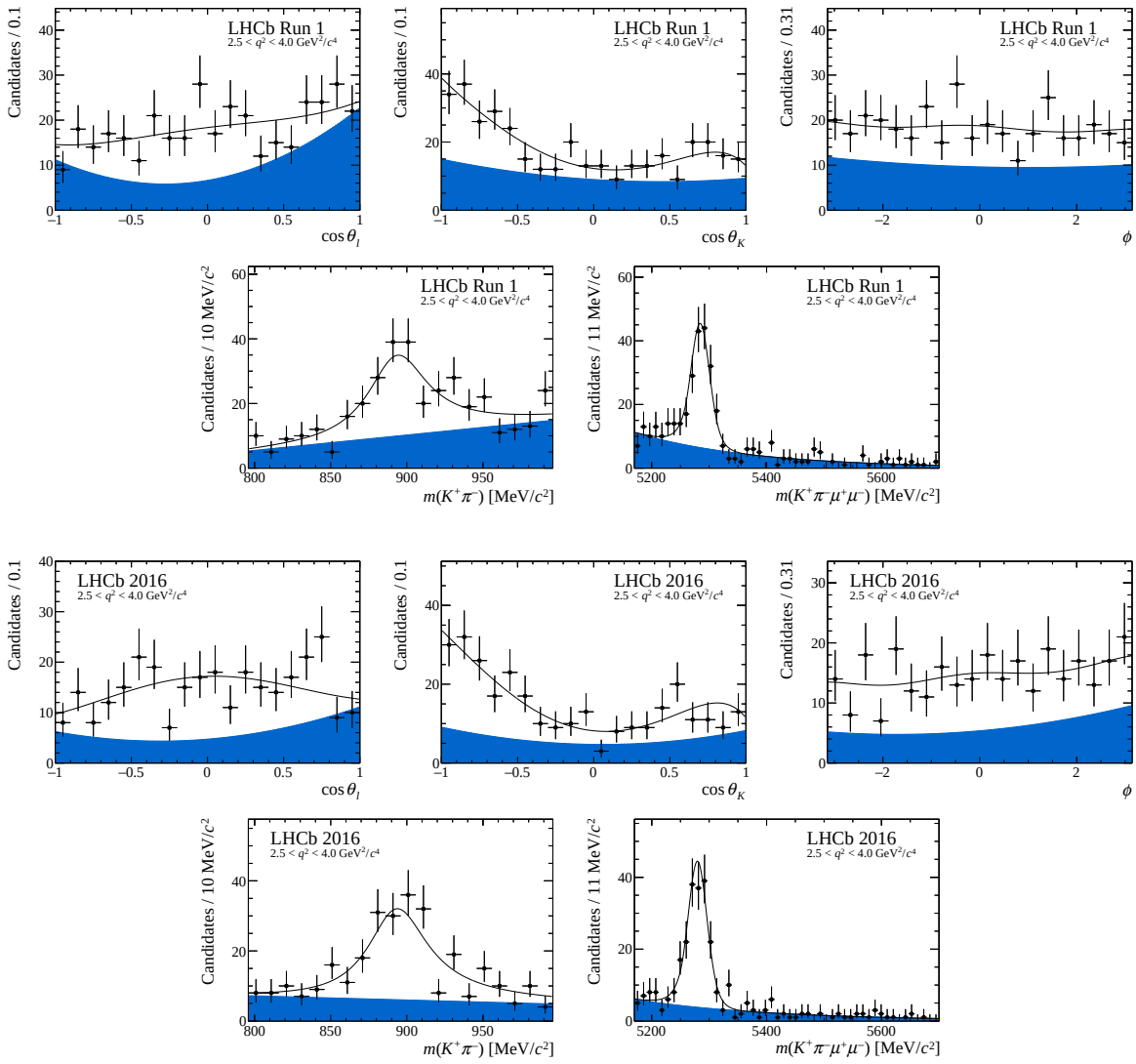

Figure 5: Projections of the fitted probability density function on the decay angles, $m(K^+\pi^-)$ and $m(K^+\pi^-\mu^+\mu^-)$ for the bin $2.5 < q^2 < 4.0\,\mathrm{GeV}^2/c^4$. The blue shaded region indicates background.

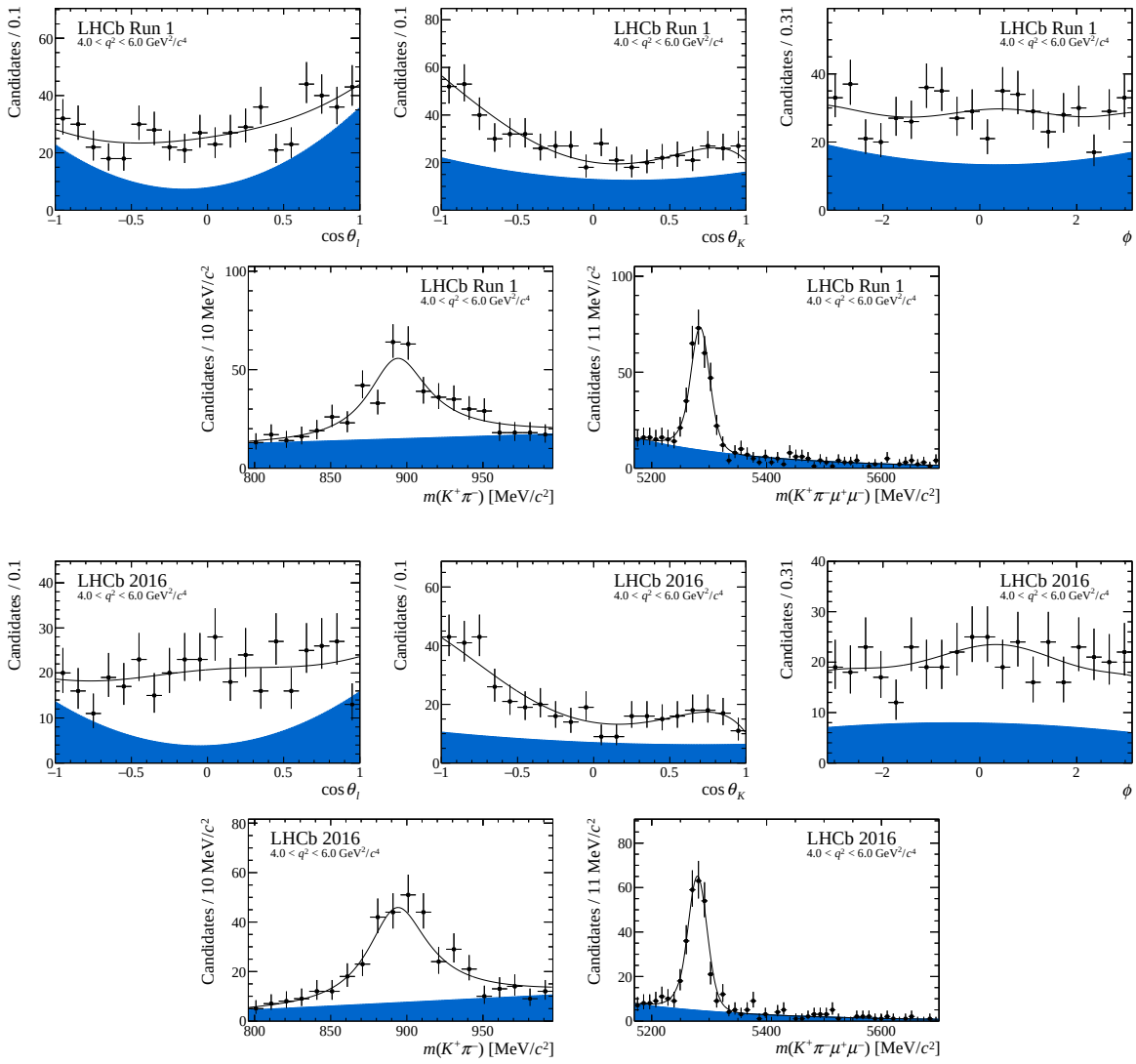

Figure 6: Projections of the fitted probability density function on the decay angles, $m(K^+\pi^-)$ and $m(K^+\pi^-\mu^+\mu^-)$ for the bin $4.0 < q^2 < 6.0\,\mathrm{GeV}^2/c^4$. The blue shaded region indicates background.

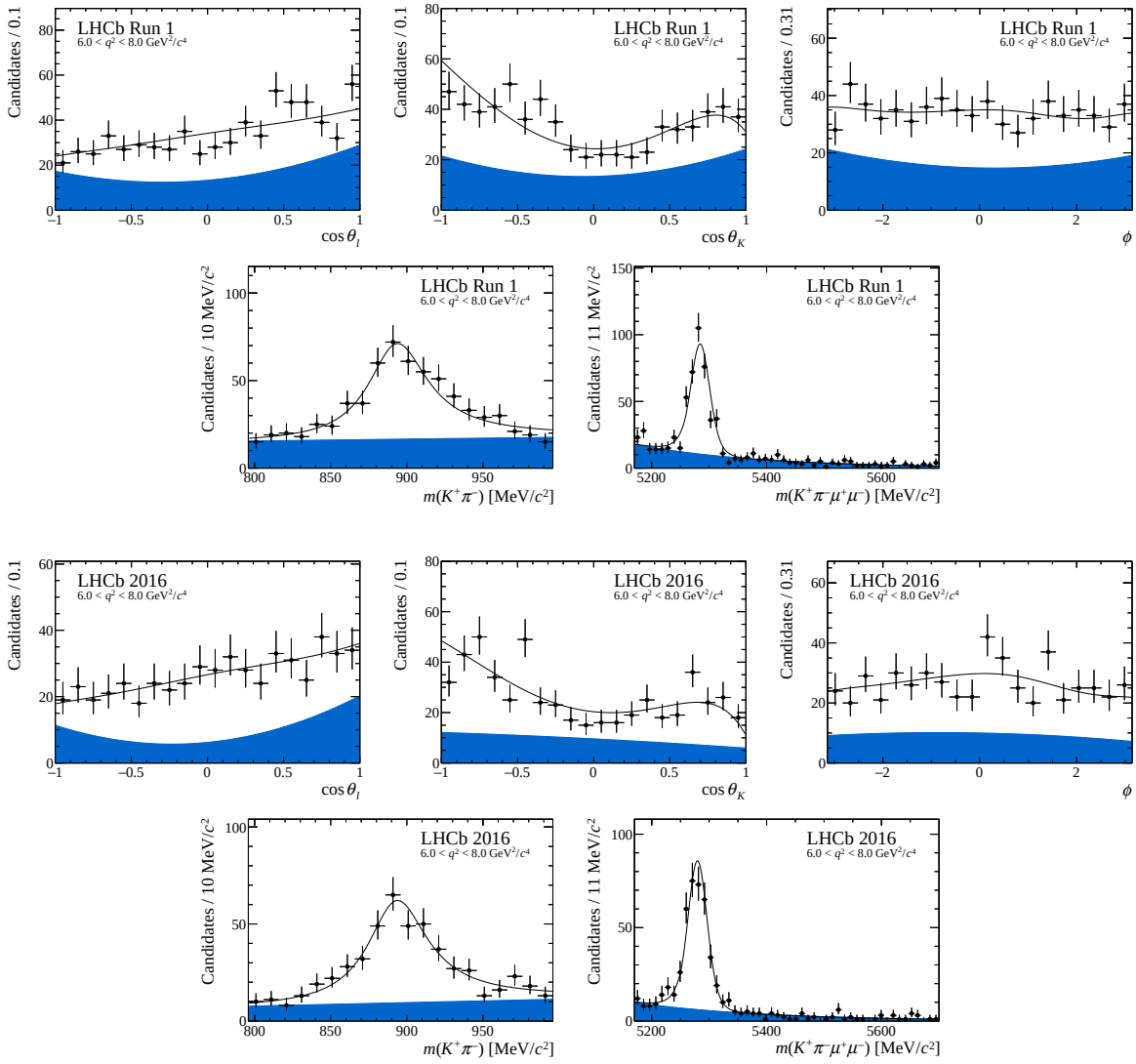

Figure 7: Projections of the fitted probability density function on the decay angles, $m(K^+\pi^-)$ and $m(K^+\pi^-\mu^+\mu^-)$ for the bin $6.0 < q^2 < 8.0\,\mathrm{GeV}^2/c^4$. The blue shaded region indicates background.

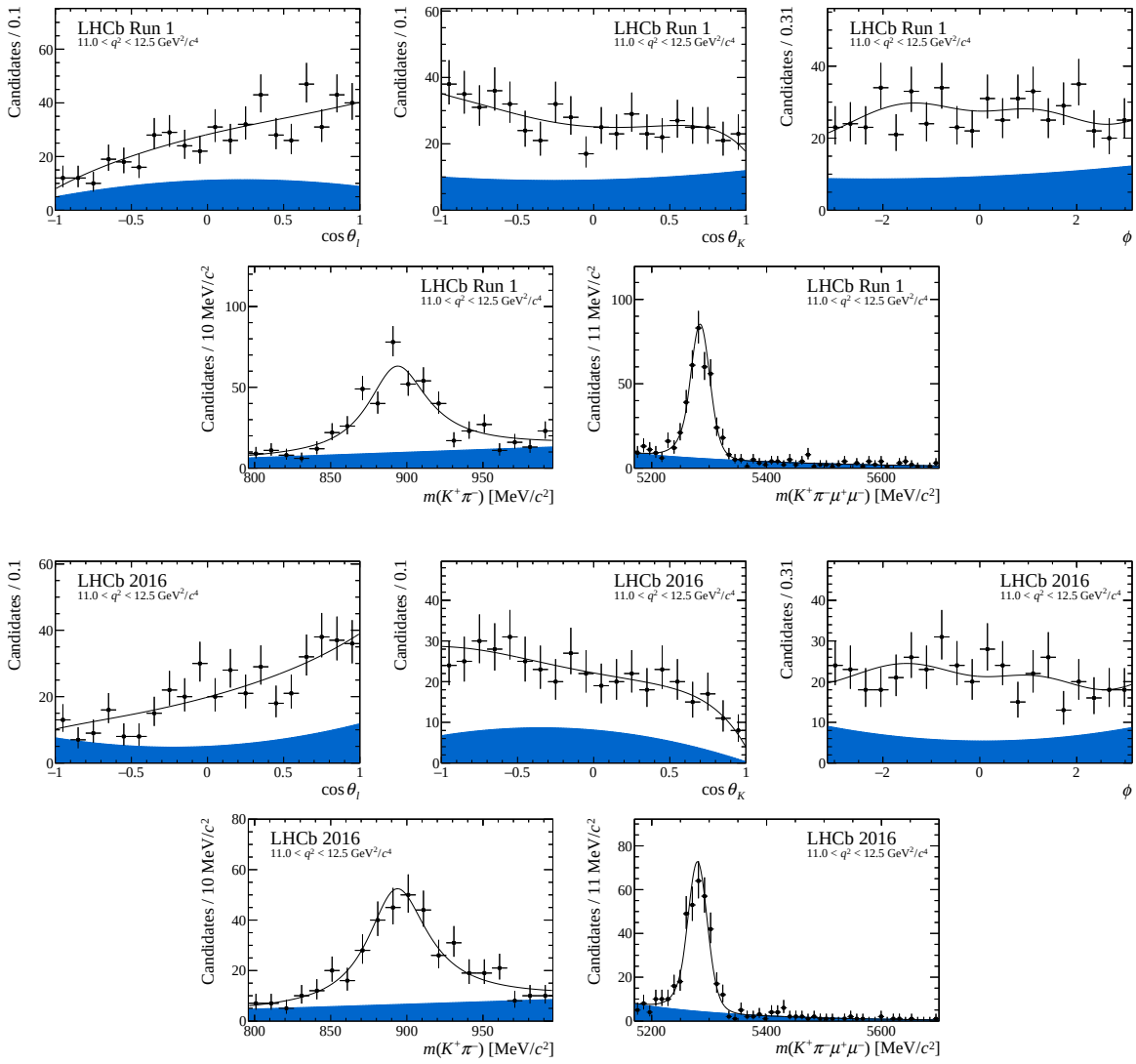

Figure 8: Projections of the fitted probability density function on the decay angles, $m(K^+\pi^-)$ and $m(K^+\pi^-\mu^+\mu^-)$ for the bin $11.0 < q^2 < 12.5\,\mathrm{GeV}^2/c^4$. The blue shaded region indicates background.

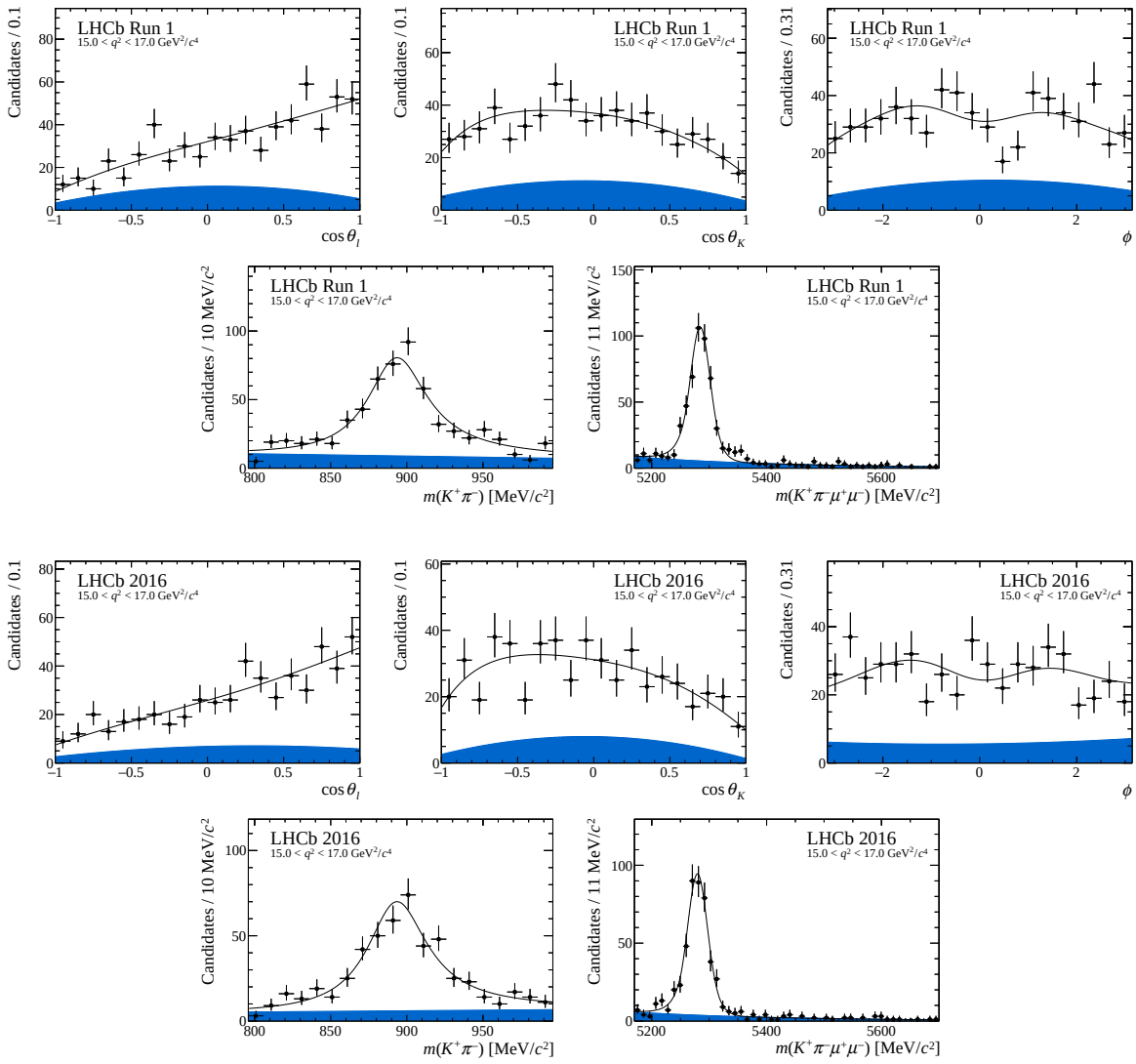

Figure 9: Projections of the fitted probability density function on the decay angles, $m(K^+\pi^-)$ and $m(K^+\pi^-\mu^+\mu^-)$ for the bin $15.0 < q^2 < 17.0\,\mathrm{GeV}^2/c^4$. The blue shaded region indicates background.

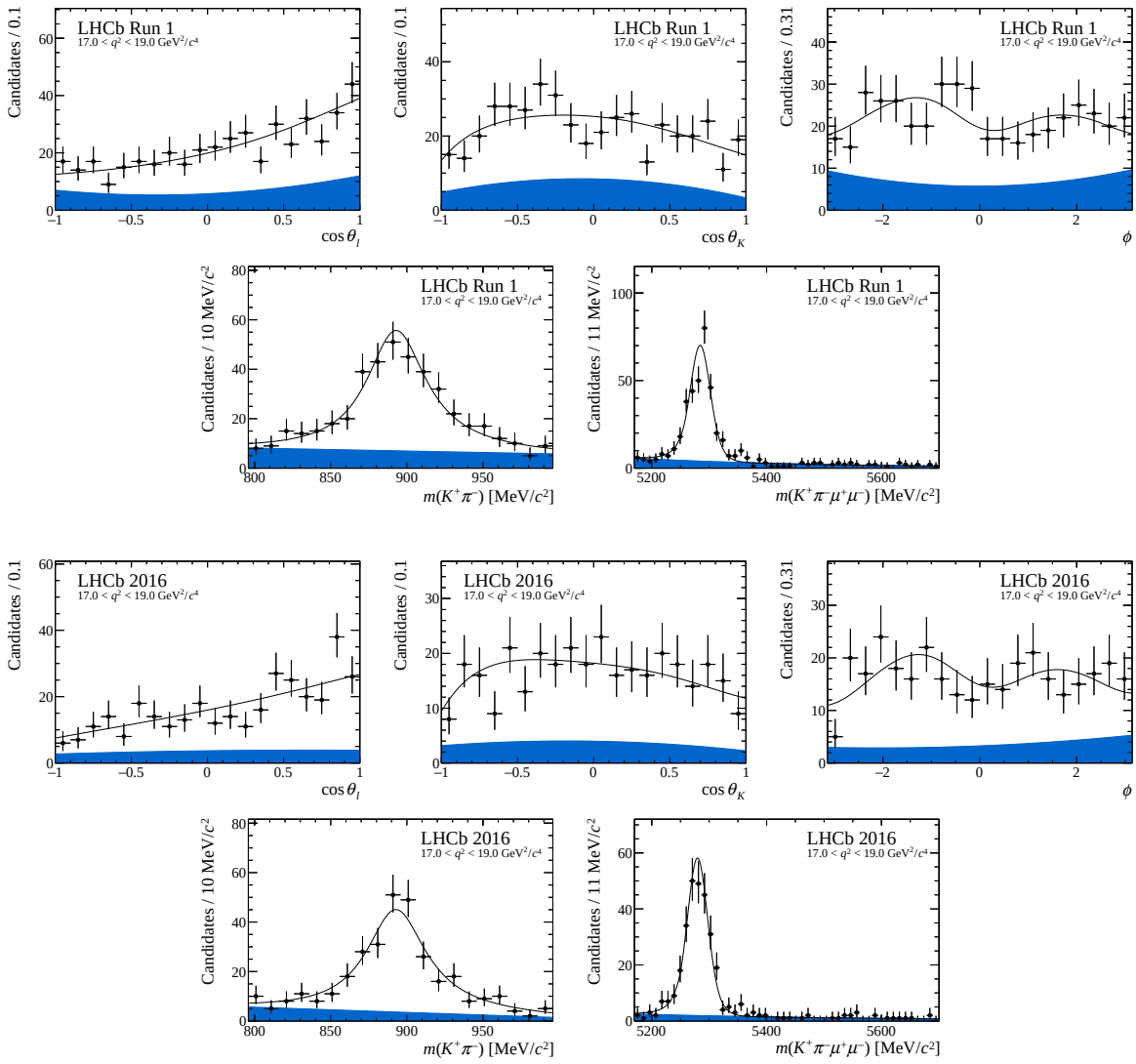

Figure 10: Projections of the fitted probability density function on the decay angles, $m(K^+\pi^-)$ and $m(K^+\pi^-\mu^+\mu^-)$ for the bin $17.0 < q^2 < 19.0\,\mathrm{GeV}^2/c^4$. The blue shaded region indicates background.

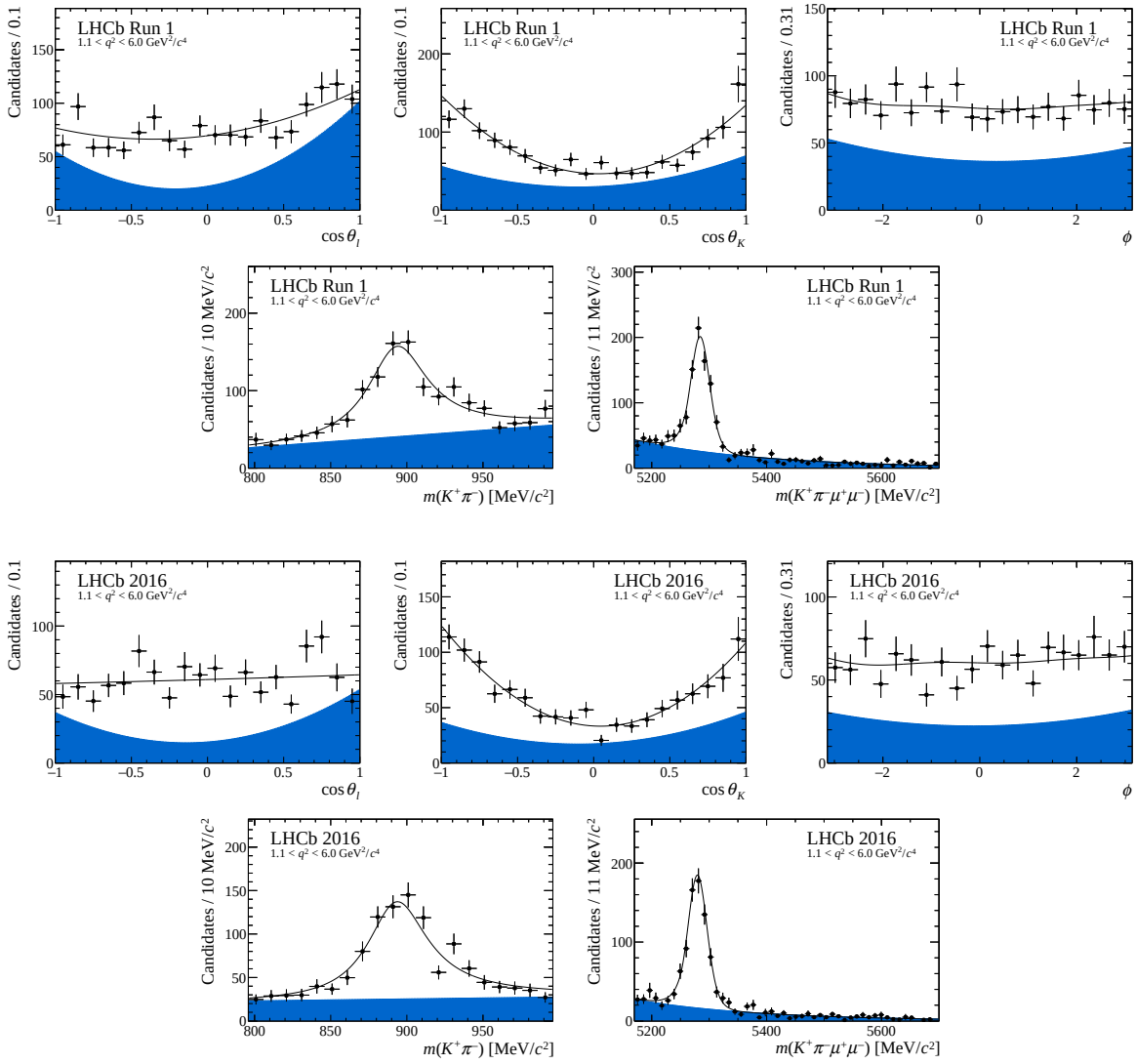

Figure 11: Projections of the fitted probability density function on the decay angles, $m(K^+\pi^-)$ and $m(K^+\pi^-\mu^+\mu^-)$ for the bin $1.1 < q^2 < 6.0\,\mathrm{GeV}^2/c^4$. The blue shaded region indicates background.

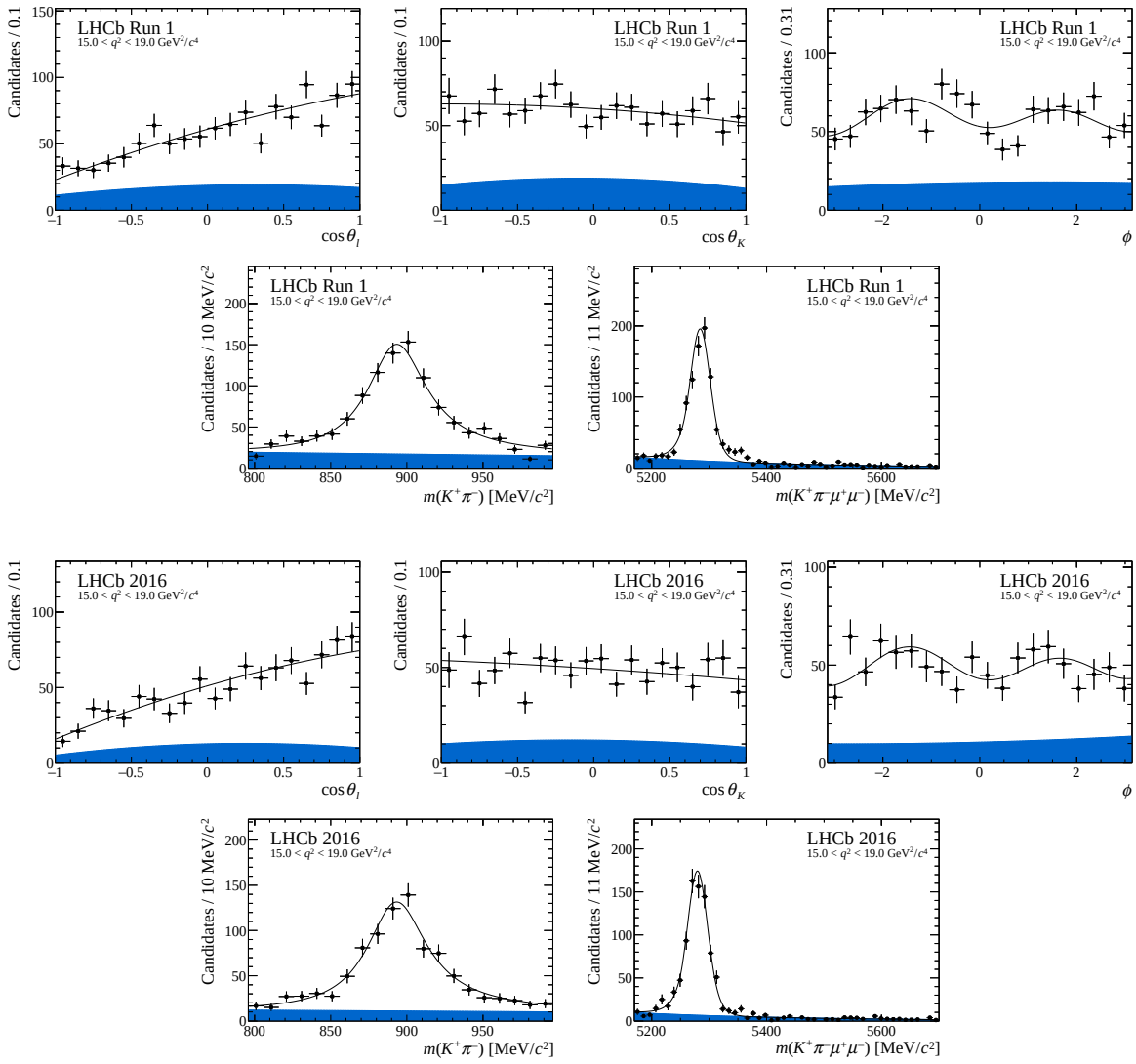

Figure 12: Projections of the fitted probability density function on the decay angles, $m(K^+\pi^-)$ and $m(K^+\pi^-\mu^+\mu^-)$ for the bin $15.0 < q^2 < 19.0\,\mathrm{GeV}^2/c^4$. The blue shaded region indicates background.

References

[1] W. Altmannshofer and D. M. Straub, *New physics in $b \to s$ transitions after LHC run 1*, Eur. Phys. J. **C75** (2015) 382, arXiv:1411.3161.

[2] A. Bharucha, D. M. Straub, and R. Zwicky, *$B \to V\ell^+\ell^-$ in the Standard Model from light-cone sum rules*, JHEP **08** (2016) 098, arXiv:1503.05534.

[3] R. R. Horgan, Z. Liu, S. Meinel, and M. Wingate, *Lattice QCD calculation of form factors describing the rare decays $B \to K^*\ell^+\ell^-$ and $B_s \to \phi\ell^+\ell^-$*, Phys. Rev. **D89** (2014) 094501, arXiv:1310.3722.

[4] R. R. Horgan, Z. Liu, S. Meinel, and M. Wingate, *Rare B decays using lattice QCD form factors*, PoS LATTICE2014 (2015) 372, arXiv:1501.00367.

[5] S. Descotes-Genon, L. Hofer, J. Matias, and J. Virto, *On the impact of power corrections in the prediction of $B \to K^*\mu^+\mu^-$ observables*, JHEP **12** (2014) 125, arXiv:1407.8526.

[6] A. Khodjamirian, T. Mannel, A. A. Pivovarov, and Y.-M. Wang, *Charm-loop effect in $B \to K^{(*)}\ell^+\ell^-$ and $B \to K^*\gamma$*, JHEP **09** (2010) 089, arXiv:1006.4945.